energies

MDPI

Article

Smart Meter Data-Based Three-Stage Algorithm to Calculate Power and Energy Losses in Low Voltage Distribution Networks †

Gheorghe Grigoras * and Bogdan-Constantin Neagu

Department of Power Engineering, "Gheorghe Asachi" Technical University of Iasi, Iasi 700050, Romania

* Correspondence: ggrigor@tuiasi.ro or ghgrigoras@yahoo.com; Tel.: +04-0232-278-683

† This paper is an extended version of our paper published in: "Grigoras, G.; Gavrilas M. An Improved Approach for Energy Losses Calculation in Low Voltage Distribution Networks based on the Smart Meter Data, presented at the Proceedings of 10th International Conference and Exposition on Electrical and Power Engineering (EPE), Iasi, Romania, 2018, pp. 749–754".

Received: 23 June 2019; Accepted: 2 August 2019; Published: 4 August 2019

Abstract: In this paper, an improved smart meter data-based three-stage algorithm to calculate the power/energy losses in three-phase networks with the voltage level below 0.4 kV (low voltage—LV) is presented. In the first stage, the input data regarding the hourly active and reactive powers of the consumers and producers are introduced. The powers are loaded from the database of the smart metering system (SMS) for the consumers and producers integrated in this system or files containing the characteristic load profiles established by the Distribution Network Operator for the consumers, which have installed the conventional meters non-integrated in the SMS. In the second stage, a function, which is based on the work with the structure vectors, was implemented to easily identify the configuration of analysed networks. In the third stage, an improved version of a forward/backward sweep-based algorithm was proposed to quickly calculate the power/energy losses to three-phase LV distribution networks in a balanced and unbalanced regime. A real LV rural distribution network from a pilot zone belonging to a Distribution Network Operator from Romania was used to confirm the accuracy of the proposed algorithm. The comparison with the results obtained using the DigSilent PowerFactory Simulation Package certified the performance of the algorithm, with the mean absolute percentage error (MAPE) being 0.94%.

Keywords: distribution networks; energy losses; three-stage algorithm; smart meters; characteristic load profiles

1. Introduction

Until a few years ago, electric distribution networks were generally characterized by a lack of technical possibilities represented by smart devices that can help the Distribution Networks Operators (DNOs) in the supervisory, control, and decision-making processes. Although the low voltage (LV) distribution networks feed a high number of consumers, little information could be gathered from inside (from the consumers and producers), with a delayed response time. In order to obtain as much data as possible from the network, it is necessary to install smart meters, which allow the recording of the supervised data (energy consumptions, active and reactive powers, voltages, power factors, harmonics etc.) and their transmission to the DNOs level.

The Smart Metering technology is essential for achieving targets regarding the energy efficiency and renewable energy set for 2020, as well as the delineation of future smart grids. The introduction of smart metering systems (SMS) in the European Union is finished in some countries and it is in different stages in others [1–5]. Thus, special attention should be paid to the management of databases built

with the help of information provided by smart meters from consumers and producers for improving the energy efficiency in LV distribution networks. The benefits of smart meters consist of the fact that, in addition to the metering function, they also provide a whole range of applications such as the following [6,7]:

- Secure transmission of data to the consumers, the DNOs, or another operator (for example Metering Operator);
- Bidirectional communication between the smart meters installed at consumer/producers and the data concentrators (information management points) belonging to the DNO;
- Remote controlled connection/disconnection from the network or demand limitation at the consumers;
- Implementing differentiated time-of-use tariffs.

In these circumstances, the DNOs can obtain accurate online information regarding the energy consumptions and productions from the renewable sources, which allows them to calculate the energy losses and then to take some technical measures which will enable the low voltage networks to operate more energy efficiently and better plan their investments. For LV electrical networks, the information needed to calculate the power and energy losses is easily obtained if consumers are integrated into the SMS. In this context, the DNOs should use accurate methods and take into account all components (lines and transformers) in order to have a correct evaluation regarding the efficiency of their own LV distribution networks. Thus, an accurate analysis of the steady-state regimes corresponding the LV distribution network can be made through real-time monitoring using the smart meters. Based on the recorded data, the following state variables could be immediately determined: The current flows in each line section, the voltage in all nodes, and the power and energy losses in the all network elements and in the whole network.

More methods are presented in the literature to estimate the power/energy losses, but unfortunately, the loss factor formulas represent the support of them. For example, the statistical data determined from the active power profiles (the average value and the standard deviation) were used in Reference [8] to calculate the loss factor in order to estimate the energy losses. A similar approach, based on the average value and the variation limits of the required power by consumers, extracted from active power profiles, was proposed in Reference [9]. The load profiles and some primary variables of medium voltage (MV) feeders, which refer at the length, the loading factor at the peak load, and a distribution function of the load, have constituted the data used in Reference [10] for the simulation studies, in order to determine the repartition functions of power losses at the maximum loading. The difference between the incoming and outgoing energy amounts from the distribution network represents another approach to evaluate energy losses, presented in Reference [11]. Additionally, the loss factors were calculated in Reference [12] and Reference [13] to evaluate the energy losses in the distribution networks. A scaling factor was used in References [14–16] for the characteristic load profiles, with attached pseudo measurements performed in the balanced LV networks with distributed generation sources in order to estimate power losses. In Reference [17,18], the loss factor and the load profile were used to calculate the power losses. The drawback of this method is represented by the estimation of two constant coefficients, A and B, for the homogeneous loads or the load profiles. Moreover, in References [19,20] the active power losses for the balanced (neglecting the neutral) LV feeders were calculated. All the aforementioned methods used the Joule power losses estimation, a simplified methodology based on the Kirchhoff laws.

Currently, due to the large number of consumers connected to the LV networks (for example, in Romania there are over 9 million consumers), the implementation of SMS was not done to 100% in all European countries, until now. There are countries where the implementation of this system is at the end, while others are at the beginning or in different intermediate stages. As a result, there is a high degree of uncertainty about the active and reactive powers of consumers and, consequently, about the loading level of network, the voltage level, and the power losses. In addition, the DNOs do not record

all data regarding the LV feeders from the MV/LV electric substations (the number of these distributors are very high), as there are uncertainties over the lengths or cross-sections of conductors. All these effects from the uncertainties is propagated in the calculations of the steady-state regime. Artificial intelligence techniques can be considered as a suitable means in the above cases of uncertainties in order to model the material characteristics of the networks and the loads. Thus, the similarity between the load characteristics of feeders based on clustering techniques was used in Reference [21] to assess the power/energy losses in the LV networks. A similar approach is proposed in Reference [22], but the difference is represented by the following considered variables: The voltage level (6, 10, or 20 kV), the rated power of transformers, the available distribution substations (MV/LV), and the loading degree of the feeders. A hybrid approach was proposed in Reference [23], which considered the use of a hierarchical clustering algorithm and an improved gradient algorithm. The primary technical variables and load characteristics of each feeder are obtained from the databases of the DNO. A genetic algorithm-based approach regarding power loss computations for a LV distribution network was proposed in Reference [24]. The total active power losses are considered as a sum of power losses computed for the phase and neutral conductors (a, b, c, and 0). The particularity of the method refers to consumers, defined through the installed active and reactive powers, the utilization factor, the phase allocation, and the connection at the pillar.

Unlike the above approaches, the proposed algorithm has the following advantages identified in each stage:

- *Stage I* is based on the online work, with files from two different databases, as follows: The database of the SMS, including the consumption and production profiles for the integrated consumers and producers and the database containing the characteristic load profiles (CLPs) obtained from the profiling process, which are assigned to the consumers with installed conventional meters, non-integrated in the SMS. This work mode enables the algorithm to work online to estimate the power losses.
- *Stage 2* implements a recognition function of the network topology based on two structure vectors.
- *Stage 3* is based on an improved version of a forward/backward sweep-based algorithm to quickly calculate fast the power/energy losses in three-phase LV distribution networks with balanced and unbalanced operating regimes. Regarding the forward/backward sweep-based algorithm, it was mainly used in the medium voltage distribution networks to calculate the balanced symmetric steady-state regime [25–28]. However, the proposed version was adapted to the LV distribution networks that most often operate in unbalanced regimes due to the chaotic allocation of the single-phase consumers on the phases.

Taking into account the aforementioned references, a brief characterization taking into account the two main advantages (the online estimation of the power losses and the consideration of the unbalance regime) of the proposed algorithm compared with some other approaches is presented in Table 1.

There is not a discussion about online estimation of power losses in any paper, very few papers treat the unbalanced regime, and the simultaneous consideration of both advantages is not addressed.

Besides the two main advantages, our algorithm uses real data regarding the active and reactive powers for both consumers and small-scale sources integrated in the LV distribution networks. Additionally, the calculation of the power/energy losses is made using a modified branch and bound (forward backward sweep) method. A pilot LV distribution network, from a rural area belonging to a DNO from Romania, was chosen to demonstrate the performance of the proposed algorithm.

Table 1. Comparison of the proposed algorithm with some other approaches.

Number of Reference	Objective Function	Online Estimation	Unbalanced Regime
[8,10,12,13,17,18,23]	Loss estimation using loss factor and load profile	No	No
[9]	Loss estimation using Elgerd's power loss formulas	No	No
[11,19,20]	Joule Loss estimation	No	No
[14,24]	Loss estimation using load factor	No	Yes
[15,16]	Loss estimation using scaling factor for load profile	No	No
[21,22,24]	Loss estimation based peak load duration	No	No
[25–28]	Loss estimation using the backward/forward method	No	No
[28,29]	Loss estimation with losses factor, load factor and load profile	No	Yes

A comparison with the results obtained using the DigSilent PowerFactory (DSPF) simulation package certified the accuracy of algorithm. Even if the DSPF package is one of the most powerful packages in processes simulations from the generation, transmission, and distribution levels, it presents some disadvantages. In the DSPF Simulation Package the implementation of the LV electrical network, in the form of a scheme and an individual introduction of elements (bus, line, transformer, load) represented by conventional symbols in order to perform the calculations of steady-state regimes, is necessary. The general and electrical parameters must be entered separately in the graphic interfaces, which are different in function by element. In addition, the active and reactive power profiles for each consumer and producer must be read from more comma-separated values (CSV) files that have a specific format. To build this format, the user should process supplementary files from the SMS and files with CLPs, which leads to increased calculation time and the inability to work online.

The structure of paper is organized as follows: Section 2 reveals the stages of the proposed algorithm, detailing the load profiling process used for the non-integrated consumers in the SMS, Section 3 presents the results obtained in the case of a LV network from a pilot rural zone of a DNO from Romania and a comparison with simulations made using the DSPF package, and Section 4 highlights the conclusions and the future works.

2. Three-Stage Algorithm to Calculate Power/Energy Losses

Steady-state regime calculations using the very well-known iterative methods (Seidel–Gauss or Newton–Raphson), in order to obtain power/energy losses, can be difficult to perform for LV distribution networks. This occurs due to the following particular features: The ill-conditioning given by the radial topologies, resistance with high values, and reactance with small values (depending on the cross-sections of conductors), which often operate in the unbalanced regimes due to the chaotic allocation of the single-phase consumers on the phases.

Taking into account the above features, a different approach to eliminate these drawbacks, based on the three-stage algorithm, is presented as follows:

- *Stage 1.* The input data of the consumers, referring to the energy characteristics, are read from the databases of the DNO, which contain the load profiles of each consumer integrated in the SMS or the CLPs, if the consumer has a conventional meter non-integrated in the SMS. Additionally, the production profiles of the producers from the network are loaded by the algorithm.

- *Stage 2*. The architecture of network is established using an efficient algorithm based on two structure vectors.
- *Stage 3*. The power/energy losses are determined using an improved variant forward/backward sweep algorithm, which can work in the balanced and unbalanced operating regimes, with or without distributed generation.

2.1. The First Stage

Whatever the type of consumer (residential, commercial, or industrial), they have their own consumption pattern, which can be identified based on a load profile representing the consumed active and/or reactive power in a time frame. However, access to these data can be available only if the consumer is integrated in the SMS. In this regard, the vast majority of the DNOs from the UE countries implemented pilot projects to identify the efficiency of the integration in the SMS of the consumers. The expected results should refer to the following [1]:

- The energy consumption is monitored online with benefits for both parts, the DNOs can implement the energy efficiency measures, and the consumers can establish their pricing mode in function by the energy consumption behaviour.
- The analysis of recorded data must lead to optimal strategies regarding the increase of energy efficiency in the LV distribution networks of the DNOs.
- Extending the processed data (as load type profiles) to the networks from the same area, but without SMS implementation, to analyse their operation regime.

The algorithm accepts the input data using an available format in the database of the DNOs. The records with the associated fields from the input file are indicated in Table 2.

Table 2. The format of input data.

Number	Pillar	Branching	Phase	Type	Class	Integration	Meter ID
1	1	1-P	b	1	3	1	3002864374
2	2	1-P	b	1	1	1	3002864354
3	2	1-P	c	2	1	1	3002864393
4	3	3-P	abc	1	1	1	3002864504
-	-	-	-	-	-	-	-
N	3	1-P	b	1	1	1	3002108670

Each field of a record is detailed as follows:

- *Number* represents the allocated record for a certain consumer in the database of the DNO.
- *Pillar* represents the identification number of each pillar made by the DNO for a rural LV distribution network. The pillars are numbered in all rural LV distribution networks to know where the consumers are connected. For example, in Table 1 consumer 1 is connected at pillar 1 and consumer 4 is connected at pillar 3.
- *Branching* identifies the type of electric branching for each consumer, single-phase or three-phases. These can be identified in the database with 1-P (single-phase) or 3-P (three-phases).
- *Phase* allows for identification of the phase(s) at which a consumer is allocated (the notations *a*, *b*, or *c* can be seen for a 1-P consumer, and the notation *abc* can be observed for a 3-P consumer).
- *Type* emphasizes if the consumer belongs in the following consumption patterns: Residential (ID is 1); non-residential, namely community buildings, hospitals, town halls, schools, etc. (ID is 2); commercial (ID is 3); and industrial (ID is 4).
- *Class* belongs to a certain *Type*, identified by the annual electric energy consumption of the consumer. The DNO can classify the consumers in a given number of consumer classes in function

of different criteria. As an example, a division into five classes (made by a DNO from Romania) for the consumers from residential/non-residential types [28] is the following: *Class_1* (0–400 kWh), *Class_2* (400–1250 kWh), *Class_3* (1250–2500 kWh), *Class_4* (2500–3500 kWh), and *Class_5* (>3500 kWh).

- *Integration* allows the user to know if the meter is (value is equal to 1) or is not (value is equal to 0) in the database of the SMS. If the meter is integrated, based on the *ID* of the meter, the active and reactive power profiles of the consumer can be loaded from the database. If a meter is not integrated, then the daily energy indexes will be loaded from the database. In this last case, a CLP will be allocated to the consumer using the approach presented in the next section in function of the records *Type* and *Class*. The associated active and reactive power profile is finally obtained based on the loaded energy indexes.

A matrix, with a number of rows equal to the sampling size of the active and reactive power profiles (usually one hour) and a number of columns, with the size $2 \times 3 \times$ total number of consumers, is loaded. The signification of the 2×3 columns is given by the fact that three columns for the active power and three columns for the reactive power is allocated for each consumer. Only columns associated with the connection phase of the consumers will have values different by 0 in the input matrix. Additionally, the algorithm can be used in the online calculations, with the data being read as soon as they reached in the data center.

Load Profiling Process Based on Smart Meters Data

Load Profiling represents a procedure that allows the energy consumption history of consumers not equipped with smart meters to be converted into a series of estimated load profiles, named "characteristic load profiles" (CLPs), for a certain type of consumer (residential, non-residential, commercial, and industrial). Thus, through the profiling process, the total energy consumption of a consumer for a time interval (one day) is distributed at all hourly levels. CLPs are derived from the processing of active and reactive profiles, with a sampling by 1 h, on a statistical sample belonging to a consumer type (residential, non-residential, commercial, industrial) and belonging to an energy consumption class. The consumption classes are established by DNOs in function of the annual energy consumption, because this is different from consumer to consumer inside of each type. In addition, the energy consumption is influenced by the following factors: Season (winter, spring, summer, and autumn) and week days (weekend or workdays). All mentioned factors are considered in the profiling process and in the case when the consumer has a technical failure at the communication support or the smart meter or is not yet integrated in the SMS in function of consumption class, consumption type, season, and day of the wee, a CLP will be assigned to be used in the steady-state regime calculations. The profiling process can be implemented as an offline procedure (after the update of the database at the end of day) or an online procedure straight after all data are collected from the smart meters. In our approach, the process is implemented as an offline procedure. The term "load profiling" mainly refers to the use of CLPs in special procedures related to the calculations of the steady state regime.

In this context, if a consumer is not integrated in the SMS, the DNO will assign a CLP depending on the different consumer' types (residential, commercial, and public), energy consumption class, and seasons (spring, summer, autumn, and winter), which is obtained based on the available processed data from the consumers with smart meters [29,30].

Using the CLPs and the daily energy consumption for each consumer without a smart meter implemented, the load profiles could be computed using the following algorithm. The denormalized load profile at consumer *l* is calculated with the following relation:

$$P_l^{(h)} = W_l \cdot CLP_{tc}^{(h)}, \quad (1)$$

where

$P_l^{(h)}$—the denormalized load profile at consumer l for each hour $h = 1, \ldots, 24$, $l = 1, \ldots, N_c$;

tc—the type of the l-th consumer, $l = 1, \ldots, N_c$;

$CLP_{tc}^{(h)}$—the characteristic load profile for the tc type of consumer (tc can be residential, non-residential, commercial or industrial), for each hour $h = 1, \ldots, 24$;

W_l—the daily energy consumption for the consumer l;

N_c—total number of consumers without smart meter installed or with missing data in the SMS.

Next, the denormalized profiles calculated above are adjusted based on the hourly values recorded by the smart meter from the electric substation, as follows:

$$P_{tc}^{(h)} = \sum_{l=1}^{N_c} P_l^{(h)} \quad h = 1, \ldots, 24, \tag{2}$$

$$P_{SM}^{(h)} = \sum_{n=1}^{N_{SM}} P_{sm,n}^{(h)} \quad h = 1, \ldots, 24, \tag{3}$$

$$\Delta P^{(h)} = P_{tc}^{(h)} - P_m^{(h)} - P_{SM}^{(h)} \quad h = 1, \ldots, 24, \tag{4}$$

$$P_{cor,l}^{(h)} = P_l^{(h)} \cdot \left(1 + \frac{\Delta P^{(h)}}{\sum_{l=1}^{N_c} P_l^{(h)}} \right) \quad h = 1, \ldots, 24, \tag{5}$$

where

$P_m^{(h)}$—the three-phase feeder measured load profile for the analysed period;

$P_{sm,n}^{(h)}$—the active power measured with the smart meter at the consumer n, $n = 1, \ldots, N_{SM}$;

N_{SM}—the total number of consumers integrated in the SMS.

$\Delta P^{(h)}$—the deviation between the measured and computed load profiles for the analysed period;

$P_{cor,l}^{(h)}$—the denormalized load profiles adjusted by measured load profiles for the analysed period at the consumer l, for each hour $h = 1, \ldots 24$, $l = 1, \ldots, N_c$.

2.2. The Second Stage

The topology of the analysed network is very easily identified based on an approach which builds two structure vectors (VS1 and VS2). The approach is explained hereinafter.

The process allows the clustering of each section at a hierarchical level, starting with the first section. To exemplify the procedure, a radial LV distribution network with 8 nodes (pillars) and 7 sections was considered (see Figure 1). The steps for the network from Figure 1 are described below.

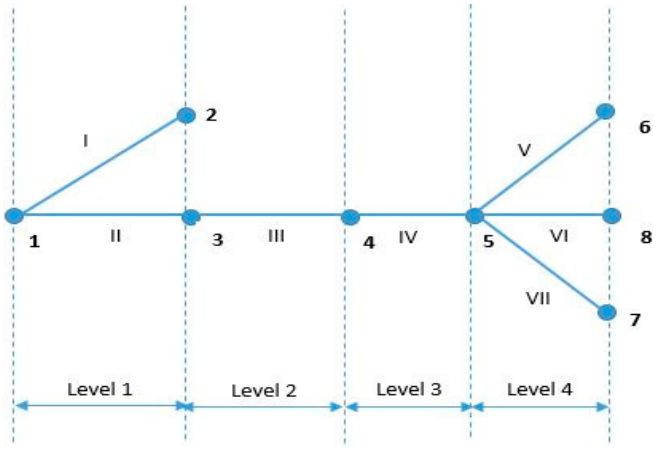

Figure 1. The topology of a radial LV distribution network.

If the following order is adopted in numbering the sections, 1–2 (I), 1–3 (II), 3–4 (III), 4–5 (IV), 5–6 (V), 5–8 (VI), and 5–7 (VII), then the size of the vector VS1 is equal with identified levels and the elements represent the sections assigned at one certain level (1, 2, 3, or 4). The correlation between vectors VS1 and VS2 can be observed in Table 3, where the structure vectors are shown.

Table 3. The structure vectors for the LV distribution network from Figure 1.

VS1	1		2	3		4	
VS2	I (1–2)	II (1–3)	III (3–4)	IV (4–5)	V (5–6)	VI (5–8)	VII (5–7)

2.3. The Third Stage

The calculations for the steady state regime from each hour, h, h = 1, . . . , H (in our case H = 24), are made using an improved variant of the forward/backward sweep algorithm, which can work both in the balanced and unbalanced regimes, with or without distributed generation. The following steps are used to calculate the power and energy losses:

Step 1. The loads from each node (pillar) are aggregated for all consumers using n^i_c, allocated at the pillar i. On each phase, {p} = {a, b, c}, the data are loaded from the database of the SMS or result from the profiling process, as follows:

$$P_i^{\{p\}} = \sum_{j=1}^{n_c^i} P_j^{i\{p\}},\ i = 1, \ldots, N_p,\ \{p\} = \{a, b, c\}, \tag{6}$$

$$Q_i^{\{p\}} = \sum_{j=1}^{n_c^i} Q_j^{i\{p\}},\ i = 1, \ldots, N_p,\ \{p\} = \{a, b, c\}, \tag{7}$$

where N_p represents the total number of pillars from the analyzed networks.

If a generator is located in a node j (it can be at the same time and the consumer), connected at the pillar i, then:

$$P_j^{\{p\}} = P_{c,j}^{i\{p\}} - P_{g,j}^{i\{p\}},\ \{p\} = \{a, b, c\}, \tag{8}$$

$$Q_j^{\{p\}} = Q_{c,j}^{i\{p\}} - Q_{g,j}^{i\{p\}},\{p\} = \{a, b, c\}, \tag{9}$$

where $P_{g,j}^{i\{p\}}$,$Q_{g,j}^{i\{p\}}$ are the active and reactive power injected by the generator from the node j, connected at the pillar i, on the phases p = {a, b, c} and $P_{c,j}^{i\{p\}}$, $Q_{c,j}^{i\{p\}}$ are the active and reactive consumed power in the node j.

Step 2. The phase voltages are initialized at each node (pillar) from the distribution network with the recorded values on the LV side of electric substation ($\underline{U}_s^{\{p\}}$). The values could be different by the nominal voltage:

$$\underline{U}_i^{\{p\}^{(0)}} = \underline{U}_s^{\{p\}},\ i = 1, \ldots, N_p,\ i \neq s\ ,\ \{p\} = \{a, b, c\}. \tag{10}$$

Step 3. Backward sweep:

- **Step 3.1**. The currents at the level of the nodes (pillars) are calculated:

$$\underline{I}_i^{\{p\}(k)} = \frac{\underline{S}_i^{\{p\}*}}{\left(\underline{U}_i^{\{p\}*}\right)^{(k-1)}},\ k = 1, \ldots K_{max},\ i = 1, \ldots, N_p,\ \{p\} = \{a, b, c\}, \tag{11}$$

$$\underline{S}_i^{\{p\}} = P_i^{\{p\}} + j \cdot Q_i^{\{p\}}, \tag{12}$$

where k is the index of current iteration and K_{max} expresses the maximum value of iterations initially introduced by the decision maker.

- **Step 3.2**. The current flow on each section (v–i) of the network are calculated:

$$\underline{I}_{v,i}^{\{p\}(k)} = \underline{I}_{i}^{\{p\}(k)} + \sum_{n \in Next(i)} \underline{I}_{i,n}^{\{p\}(k)},\ k = 1, \ldots K_{max},\ i = 1, \ldots, N_p,\ \{p\} = \{a, b, c\}, \tag{13}$$

where v is the pillar in up stream of pillar i, Next (i) is the set of pillars next to the pillar i, and (v–i) is the section.

Step 4. Forward sweep:

- **Step 4.1**. The voltage drop on the phases {*p*} of all sections is calculated:

$$\underline{\Delta U}_{v,i}^{\{p\}(k)} = \underline{Z}_{v,i} \cdot \underline{I}_{v,i}^{\{p\}(k)} + \underline{Z}_{v,i}^{0} \cdot \underline{I}_{v,i}^{0\ (k)},\ i = 1, \ldots, N_p,\ v \neq i,\ \{p\} = \{a, b, c\}, \tag{14}$$

$$\underline{Z}_{v,i} = R_{v,i} + j \cdot X_{v,i}, \tag{15}$$

where $\underline{Z}_{v,i}$ and $\underline{Z}_{v,i}{}^{0}$ are the impedances of the phase {p} = {a, b, c} and neutral conductors (0). The value $\underline{I}_{v,i}{}^{0}$ represents the current flows on the neutral conductor.

$$\underline{I}_{v,i}^{0} = \underline{I}_{v,i}^{a} + \underline{I}_{v,i}^{b} + \underline{I}_{v,i}^{c} \tag{16}$$

- **Step 4.2**. The voltage on the phase, {p} = {a, b, c}, for each pillar, i, is calculated:

$$\underline{U}_{i}^{\{p\}(k)} = \underline{U}_{v}^{\{p\}(k)} - \underline{\Delta U}_{v,i}^{\{p\}(k)},\ i = 1, \ldots, N_p,\ v \neq i,\ \{p\} = \{a, b, c\}. \tag{17}$$

- **Step 4.3**. The total apparent power injected to the network is calculated:

$$\underline{S}_{s}^{\{p\}(k)} = \underline{U}_{s}^{\{p\}} \cdot \sum_{m \in Next(s)} \underline{I}_{s,m}^{\{p\}^{*}(k)},\ \{p\} = \{a, b, c\}. \tag{18}$$

- **Step 4.4**. Testing the stopping condition of iterative process:

$$\left| \underline{S}_{s}^{\{p\}(k)} - \underline{S}_{s}^{\{p\}(k-1)} \right| \leq \varepsilon_s,\ \{p\} = \{a, b, c\}, \tag{19}$$

where ε_S represents the imposed error by the decision maker to stop the iterative process.

Step 5. If the iterative process is finished (the relation (19) is accomplished), the power loss on each section (v–i) is calculated:

$$\underline{\Delta P}_{v,i}^{\{p\}(k)} = R_{v,i} \cdot \left(\underline{I}_{v,i}^{\{p\}(k)} \right)^2 + R_{v,i}^{0} \cdot \left(\underline{I}_{v,i}^{0\ (k)} \right)^2,\ i = 1, \ldots, N_p,\ v \neq i,\ \{p\} = \{a, b, c\}, \tag{20}$$

where $R_{v,i}$ and $R_{v,i}{}^{0}$ are the resistances of the phase and neutral conductors.

The flow-chart of the proposed algorithm with the three steps is presented in Figure 2a (the first and second stages) and Figure 2b (the third stage).

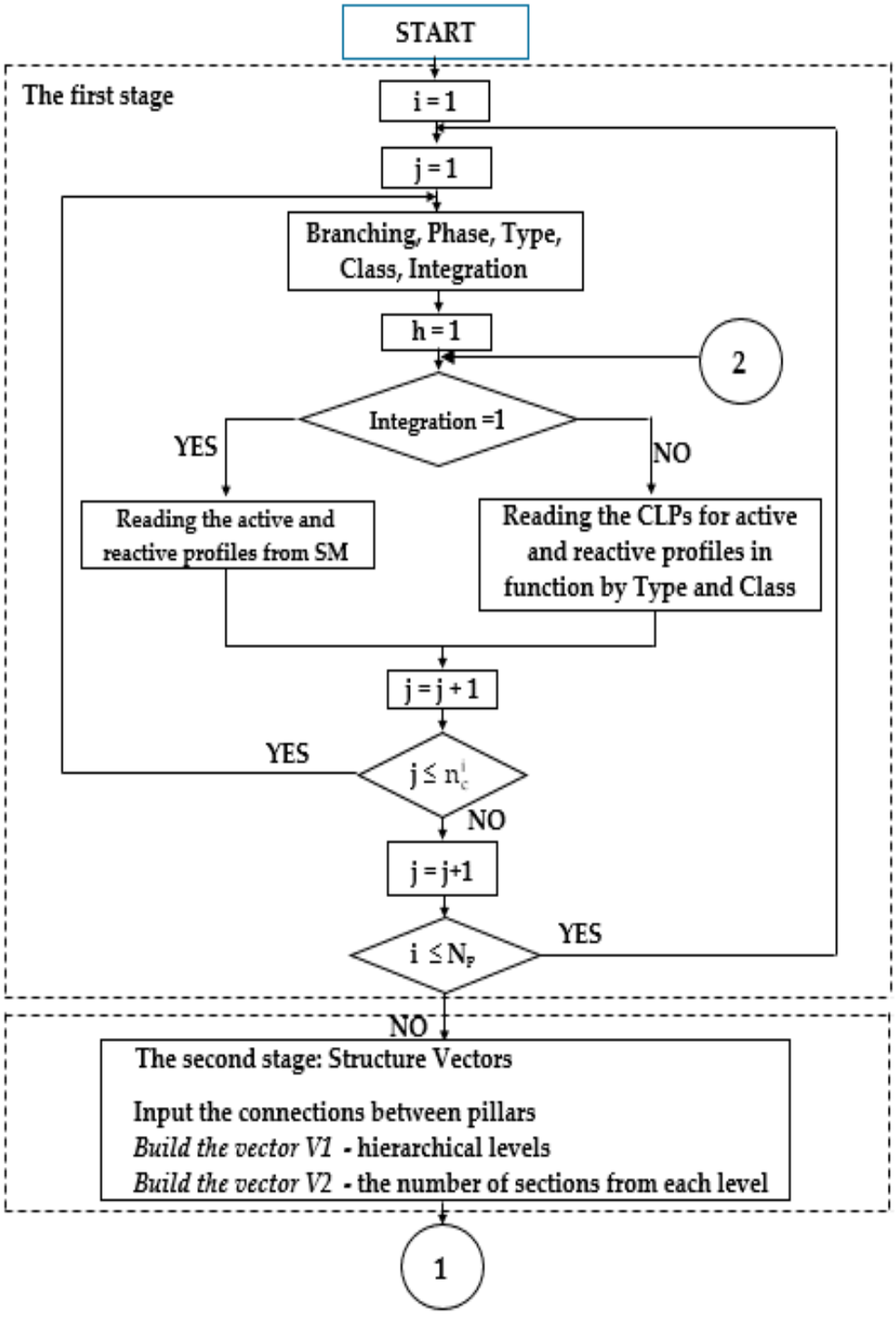

(**a**)

Figure 2. *Cont.*

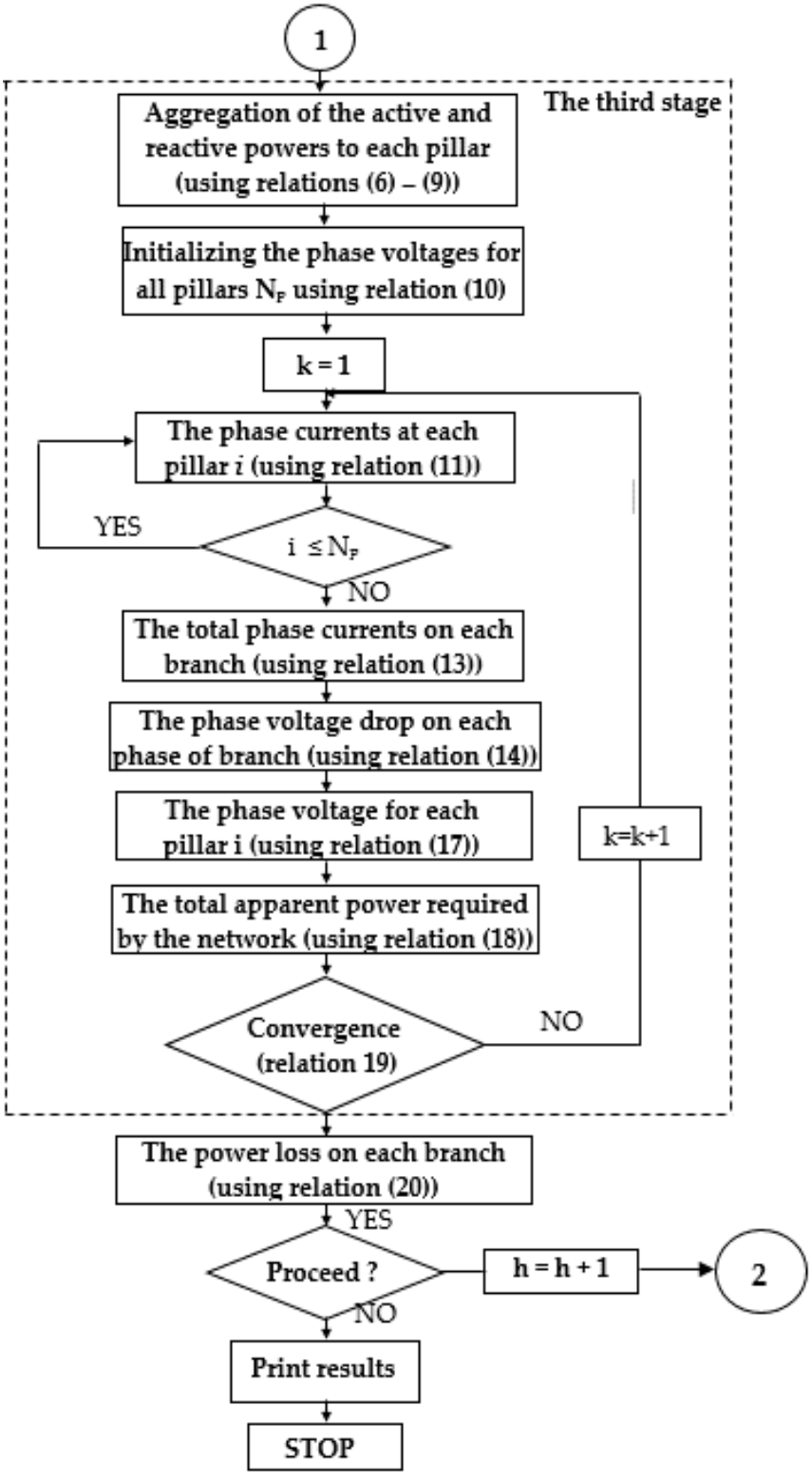

(**b**)

Figure 2. (**a**) The flow-chart of the proposed algorithm (the first and second stages); (**b**) The flow-chart of the proposed algorithm (the third stage).

3. Case Study

The proposed algorithm was tested on a real pilot LV electric distribution network belonging to a DNO from Romania. The topology of the analyzed network can be seen in Figure 3.

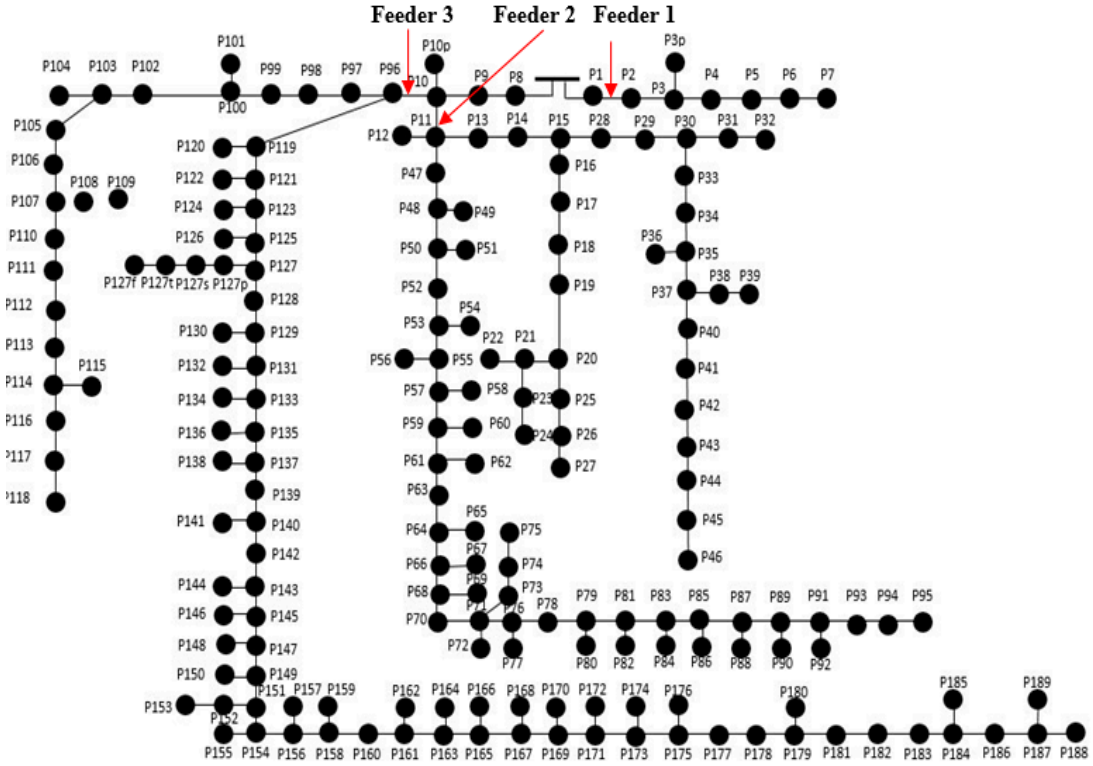

Figure 3. The analyzed LV distribution network.

The electric substation MV/LV supplies 3 distribution feeders. The three feeders have 189 pillars together. The pillars represent points where the consumers are connected using single-phase (1-P) or three-phase (3-P) branching at the network, these are identified through black circles. Each section has 40 m, representing the distance between two pillars.

The primary characteristics (number of pillars, total length, cable type, cable size, length of sections using the cable types, and the consumers' number) are shown in Table 4. Additionally, consumers' characteristics can be identified in Table 5.

Table 4. The characteristics of the feeders.

Feeder	Length [m]	Conductor Type	Cross-section (Phase + Neutral) [mm^2]	Length [m]	r_0 [Ω/km]	x_0 [Ω/km]
Feeder 1	280	Classical	1 × 50 + 50	280	0.61	0.298
Feeder 2	3880	Stranded	3 × 35 + 35	120	0.871	0.055
		Classical	3 × 50 + 50	3760	0.61	0.298
Feeder 3	3520	Stranded	3 × 50 + 50	120	0.605	0.05
		Classical	3 × 50 + 50	2080	0.61	0.298
		Classical	3 × 35 + 35	960	0.871	0.055
		Classical	1 × 25 + 25	280	1.235	0.319
		Classical	1 × 16 + 25	80	1.235	0.319
Total	7680	Classical		7440		
		Stranded		240		

Table 5. The characteristics of the consumers.

Consumers' Type		1-P	3-P
Phase a		83	-
Phase b		148	-
Phase c		104	-
Total		335	8
Consumption Class [kWh/year]	0–400	150	5
	400–1000	108	2
	1000–2500	65	0
	2500–3500	5	0
	>3500	7	1

The details regarding the allocations at pillars and phases and the type of the consumers are indicated in Appendix A, Table A1.

The connection phase of each consumer reflects the real situation and this aspect helps to establish the true-to-reality unbalanced model. The hourly load records (active and reactive power profiles) for each consumer integrated in the SMS were imported from the database of the DNO for the day when the analysis was made. Based on these profiles, the phase loading at the LV level of the electric substation was calculated for each feeder (see Figures 4–6).

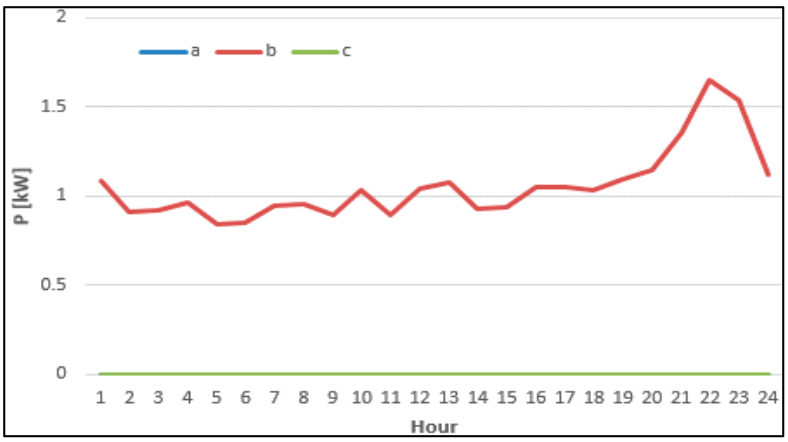

Figure 4. The phase loading on the first section of Feeder 1.

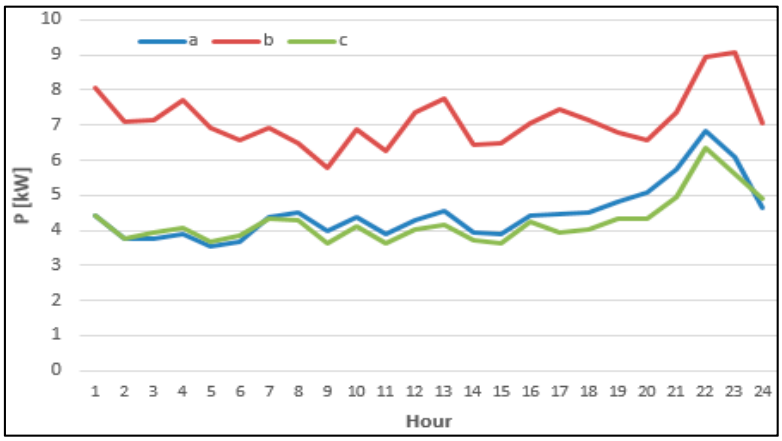

Figure 5. The phase loading on the first section of Feeder 2.

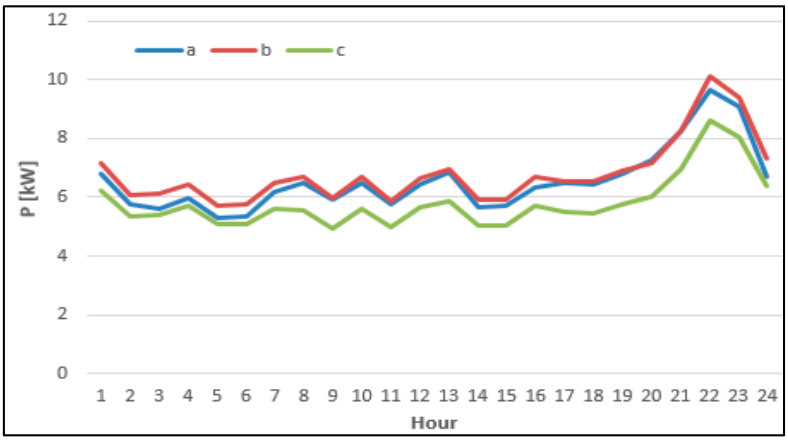

Figure 6. The phase loading on the first section of Feeder 3.

From Figure 4, it can be observed that all consumers from Feeder 1 are allocated on the phase b. Feeder 2 has a high unbalance, the phase b is more loaded than the other two phases (a and c) (see Figure 5). In this case, the current flow on the neutral conductor will lead to the high additional losses. For Feeder 3, the allocation of consumers on the phases of the feeder is more balanced (see Figure 6).

The calculations of the steady-state regime were performed at each hour, h = 1, . . . , H (where H = 24). The total energy losses calculated with the proposed algorithm for each feeder, on the phase and neutral conductors and on the branching and the main conductors are presented in Table 6. The obtained results with the DSPF software are presented in Table 7 to emphasize the accuracy of the proposed algorithm.

Table 6. The energy losses calculated with the proposed algorithm, [kWh].

Feeder		Phase			Neutral	TOTAL
		a	b	c		
Main conductors	Feeder 1	0.000	0.047	0.000	0.058	0.105
	Feeder 2	0.529	9.973	2.455	8.055	21.012
	Feeder 3	6.370	5.411	5.726	1.586	19.092
	TOTAL	6.900	15.430	8.180	9.699	40.209
Branching conductors	Feeder 1	0.000	0.006	0.000	0.004	0.010
	Feeder 2	0.055	0.173	0.019	0.162	0.410
	Feeder 3	0.072	0.052	0.052	0.086	0.263
	TOTAL	0.127	0.232	0.072	0.253	0.682
TOTAL		7.026	15.662	8.252	9.951	40.892

Table 7. The energy losses calculated with the DSPF software, [kWh].

Feeder		Phase			Neutral	TOTAL
		a	b	c		
Main conductors	Feeder 1	0.000	0.043	0.000	0.054	0.097
	Feeder 2	0.509	9.647	2.433	7.765	20.354
	Feeder 3	6.099	5.438	6.184	1.572	19.293
	TOTAL	6.608	15.129	8.616	9.391	39.744
Branching conductors	Feeder 1	0.000	0.006	0.000	0.004	0.010
	Feeder 2	0.053	0.218	0.020	0.187	0.479
	Feeder 3	0.069	0.055	0.059	0.090	0.273
	TOTAL	0.122	0.279	0.079	0.281	0.762
TOTAL		6.731	15.408	8.696	9.671	40.506

The detailed results, obtained with the proposed algorithm for each feeder, are presented in Table A2, Table A3, and Table A4 from Appendix A.

The absolute errors (ε) and percentage errors (δ) between both approaches, DSPF software, and the proposed algorithm (PA), are presented in Table 8, Figure 7, and Figure 8. The calculation relations are the following:

$$\varepsilon = |\Delta W_{DSPF} - \Delta W_{PA}|, \ [kWh], \tag{21}$$

$$\delta = \left|\frac{\Delta W_{DSPF} - \Delta W_{PA}}{\Delta W_{DSPF}}\right| \times 100, \ [\%]. \tag{22}$$

Table 8. Comparison between both approaches (the values of energy losses and the errors).

Approach		Phase			Neutral	Total
		a	b	c		
PA	[kWh]	7.03	15.66	8.25	9.95	40.89
DSPF	[kWh]	6.73	15.41	8.70	9.67	40.51
ε	[kWh]	0.3	0.25	0.45	0.28	0.38
δ	[%]	4.45	1.62	5.17	2.90	0.94

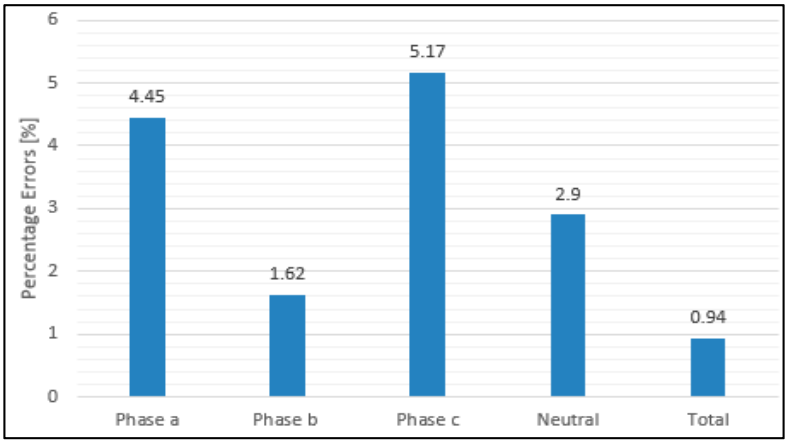

Figure 7. The errors between both approaches, [%].

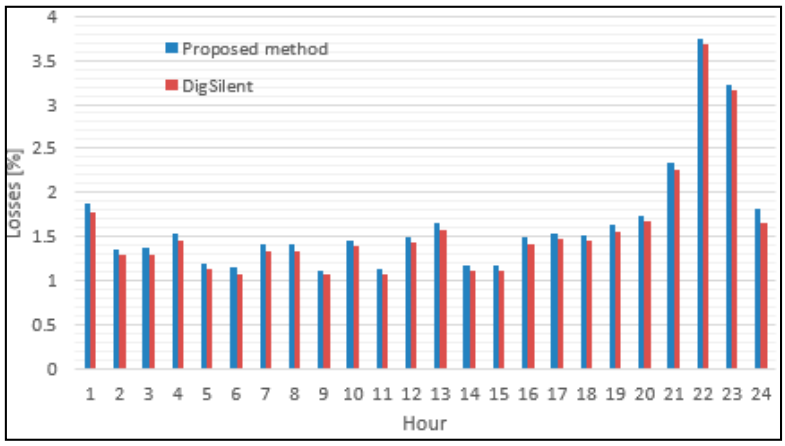

Figure 8. The hourly energy losses computed with both approaches, [%].

From Table 8, it can be observed that the percentage errors of the energy losses in conductors are in the range (1.62–5.17) and below 1 percent (0.94) for the total energy losses. In addition, a high value of energy loses in the neutral conductor can be highlighted. These represent about 25% of the total energy losses, which means that the DNO should apply the balancing measures (especially in the case of Feeder 2).

In terms of phase voltages, these were calculated for each pillar. The obtained values for the farthest pillars are represented in Figures 9–11 (pillar P95—Feeder 2) and Figures 12–14 (pillar P188—Feeder 3).

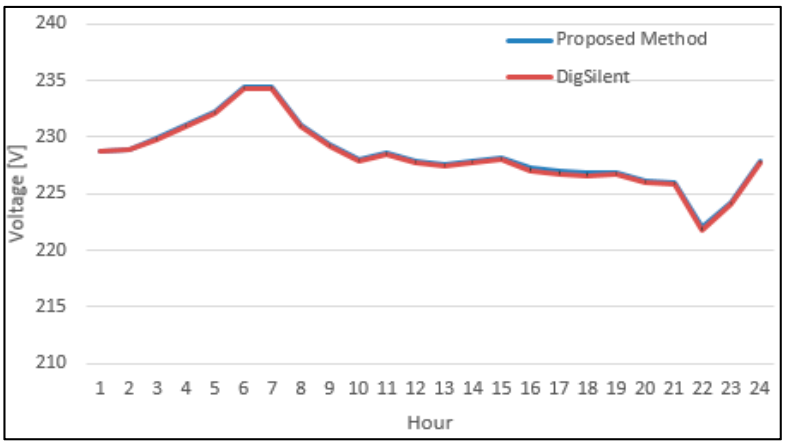

Figure 9. The phase voltage (phase a) at Pillar P95—Feeder 2.

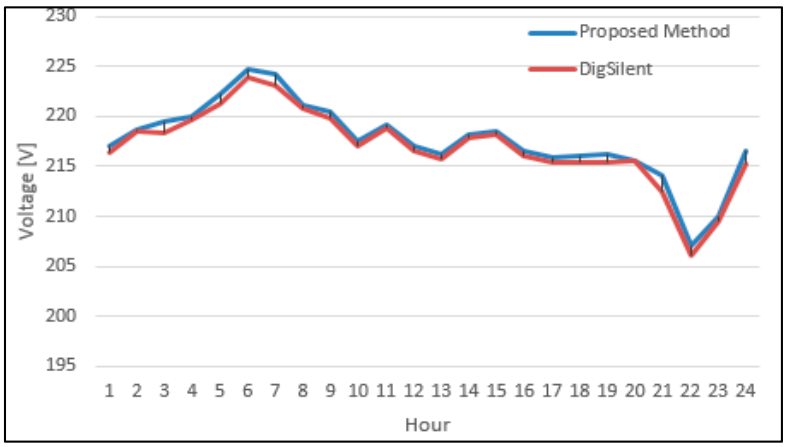

Figure 10. The phase voltage (phase b) at the Pillar P95—Feeder 2.

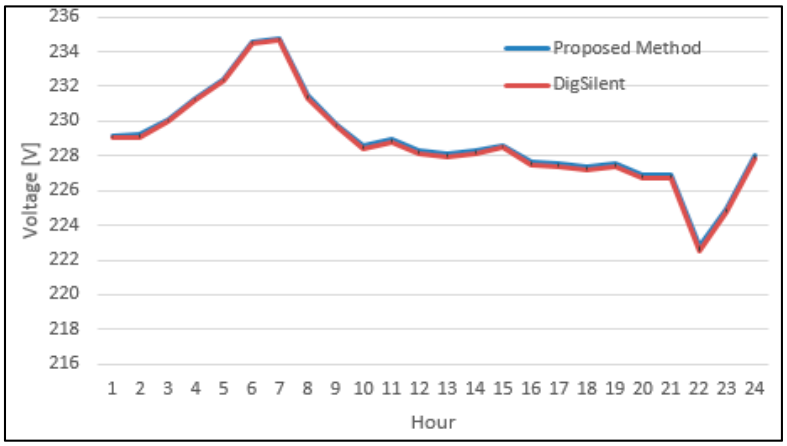

Figure 11. The phase voltage (phase c) at the Pillar P95—Feeder 2.

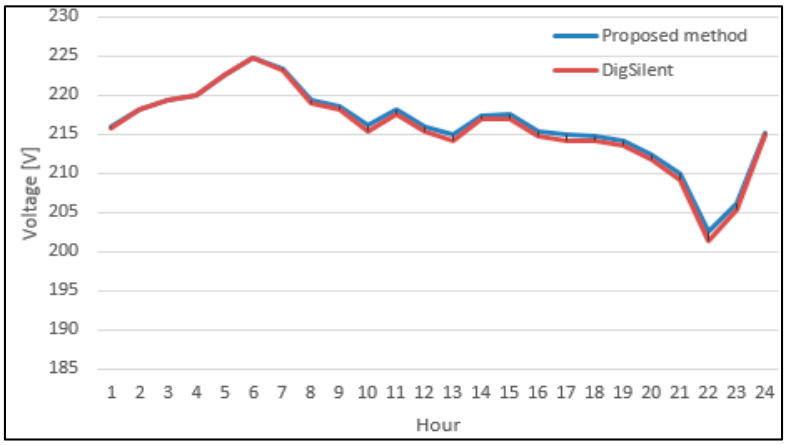

Figure 12. The phase voltage (phase a) at the Pillar P188—Feeder 3.

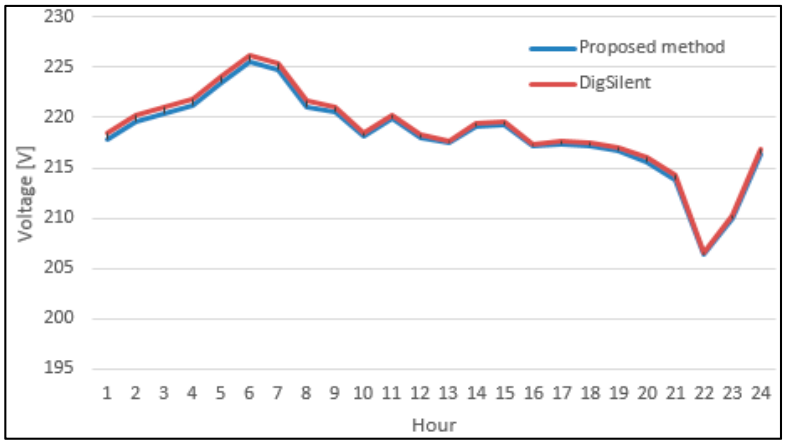

Figure 13. The phase voltage (phase b) at the Pillar P188—Feeder 3.

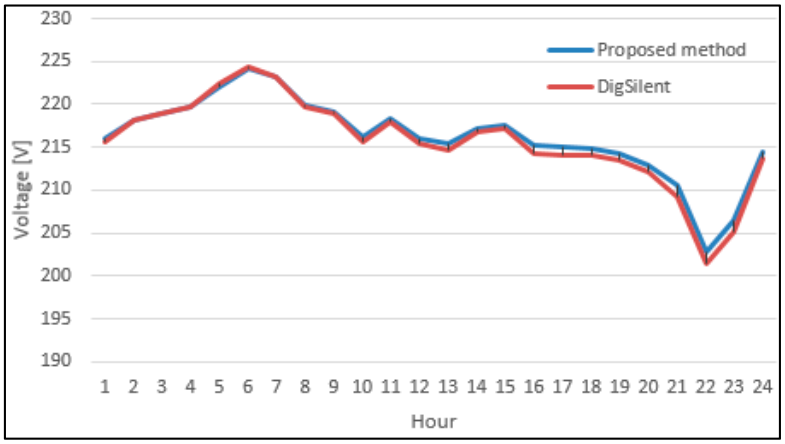

Figure 14. The phase voltage (phase c) at the Pillar P188—Feeder 3.

The detailed results obtained with the proposed algorithm for each pillar are presented in Table A5 from Appendix A.

An analysis of Figures 9–14 highlighted that at the pillar P95 the phase voltages were inside of admissible limits (nominal voltage ± 10 %) and, at the pillar P188, only the voltage on the phase b corresponded, but was equal with the minimum value (nominal voltage – 10%). The voltages on the phases a and c are slightly below the minimum limit with 0.02%. The nominal phase voltage in Romania is 230 V. Thus, the DNO should apply the measures to improve the voltage level in this final node (tap changing of transformer from the electric substation).

The mean percentage errors (MPE) of the phase voltages are presented in Figures 15 and 16. These were calculated with the following relation:

$$\mathrm{MPE} = \frac{100}{24}\sum_{t=1}^{24}\frac{\Delta W_{DSPF} - \Delta_{PA}}{\Delta W_{DSPF}}, \ [\%]. \tag{23}$$

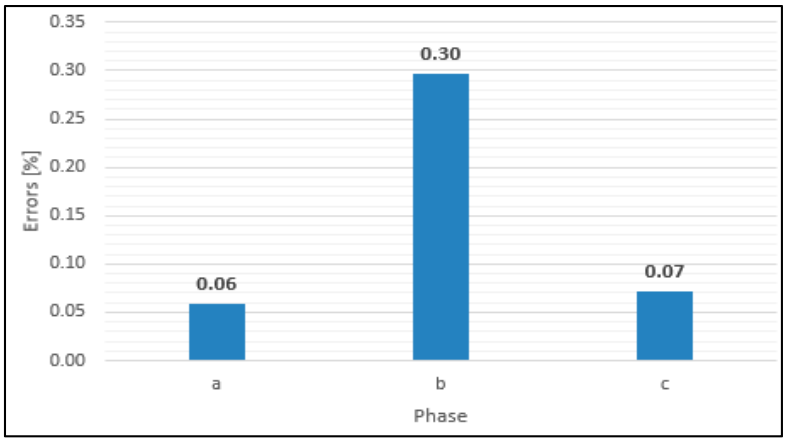

Figure 15. The MPE of the phase voltages, Pillar P95.

It can be observed that the MPEs is below 0.3 % on each phase at both pillars (P95 and P188).

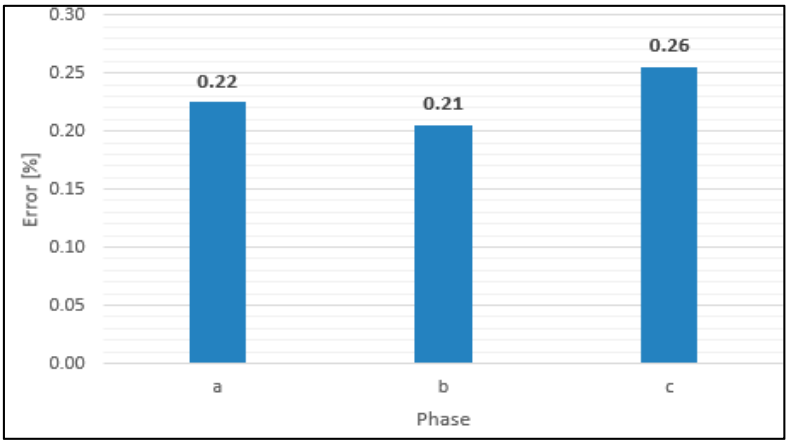

Figure 16. The MPE of the phase voltages, Pillar P188.

4. Conclusions

The paper presents an improved smart meter data-based three-stage algorithm for power/energy losses calculation in three-phase LV distribution networks. The three stages refer to the following: In *the first stage*, the data files are loaded from the databases of the DNOs, referring to the energy consumption of consumers, taking into account if they are or are not integrated in the SMS; in the *second stage*, the topological structure, based on two vectors, is identified; and in *the third stage*, the power/energy losses are calculated using an improved variant of the forward/backward sweep-based algorithm, adapted to the three-phase LV distribution networks operating in the balanced and unbalanced regimes.

The obtained results considering a pilot electric distribution network belonging to a DNO from Romania, with the consumers integrated in the SMS, were analysed and the comparison with simulations made with PFDS package software confirmed the performance of the proposed algorithm (the mean absolute percentage error was by 0.94 %). In relation to different approaches from the literature, the advantages of the proposed algorithm are the following: The comfortable introduction of network elements, whatever the size of network, and the loading of active and reactive power profiles; it works simultaneously with files containing data loaded from the database of the SMS and the CLPs assigned to consumers that have installed the conventional meters that are non-integrated in the SMS; the algorithm allows for a fast recognition of the topology based on the structure vectors; and, last but not least, algorithm allows for the elimination of difficulties due to the operation particularities of the LV distribution networks from the calculations of the steady state regime made with the classical methods (Seidel–Gauss and Newton–Raphson) using an improved version of a forward/backward sweep-based algorithm adapted to these particularities.

In addition, the algorithm can be used in online calculations, with the data being read as soon as they reach the data center. In these conditions, the DNOs have the possibility to increase the energy efficiency and to make the transition to active distribution networks. Certainly, this transition should be made step-by-step, based on the results obtained by the DNOs in the pilot zones where there are networks with the following features: Implemented SMS, installed automation devices, a management of the distributed generation, and a demand response program. The authors now work on new functions of the proposed algorithm to cover as many of the features outlined above, considering all technical constraints discussed with the decision makers of some DNOs from Romania.

Author Contributions: G.G. proposed the implementation methodology, mathematical modeling, software implementation, performed simulations, and drafted the manuscript; B.-C.N. improved the methodology and performed simulations; G.G. and B.-C.N. reviewed together the manuscript. Both authors discussed obtained results and have agreed with the structure of the paper.

Funding: This research received no external funding.

Conflicts of Interest: The authors declare no conflict of interest.

Nomenclature:

0	neutral conductor
1-P	single-phase consumer
3-P	three-phase consumer
a, b, c	phases of network
abc	three-phase consumer in the input data files
CLP	Characteristic Load Profile
DNO	Distribution Network Operator
DSPF	DigSilent Power Factory
j	The index for bus
$\underline{I}_{v,i}^{\{p\}}$	The current flow on each section (v–i), [A]
i	The index for pillar
k	The index for current iteration
K_{max}	The maximum number of iterations
h	The current hour (h = 1, . . . , H)
H	Total number of hours from the analysed period (H = 24)
LV	Low Voltage
l	The consumer non-integrated in the SMS (l = 1, . . . , N_c)
MAPE	Mean Average Percentage Error, [%]
MPE	Mean Percentage Errors, [%]
MV	Medium Voltage
n	Consumer with smart meter (n = 1, . . . , N_{SM})
N_c	Total number of consumers non-integrated in the SMS
N_P	Total number of pillars
N_{SM}	Total number of consumers integrated in the SMS
v	The pillar in up stream of pillar i
{p}	the set of phases {a, b, c}
PA	Proposed algorithm
P_g, Q_g	The active and reactive power of the generator, [kW], [kVAr]
P_c, Q_c	The active and reactive absorbed power, [kW], [kVAr]
P_l	The denormalized load profile at consumer l, [kW/kWh]
P_m	Three-phase feeder measured load profile, [kW]
P_{sm}	Active power measured with the smart meter, [kW]
P_{cor}	Denormalized load profiles adjusted by measured load profiles, [kW/kWh]
s	The LV side of electric substation
$\underline{S}_s^{\{p\}}$	The total apparent power injected to the network on the phases {p} = {a, b, c}, [kVA]
SMS	Smart Metering System
R	Resistance, [Ω]
tc	Type of consumer (residential, non-residential, commercial, and industrial)
$\underline{U}_i^{\{p\}}$	The phase voltages from each pillar i =1, . . . , N_p, [V], with {p} = {a, b, c}
$\underline{U}_s^{\{p\}}$	The phase voltages on the LV side of electric substation, [V], {p} = {a, b, c}
V1, V2	Structure vectors
$\underline{Z}_{v,i}$	The phase impedance of each section (v–i), [Ω]
$\underline{Z}_{v,i}^{0}$	The impedance of neutral conductor of each section (v–i), [Ω]
X	Reactance, [Ω]
W_l	The daily energy consumption for the consumer l = 1, . . . , N_c, [kWh]
$\Delta P^{(h)}$	The deviation between the measured and computed load profiles, [kW], at hour h = 1, . . . , H
$\Delta\underline{U}_{v,i}^{\{p\}}$	The voltage drop on the phases {p} = {a, b, c}, on each section (v–i), [V]
ΔW	The energy losses, [kWh]
ε_S	The error for the convergence test (Absolute error), [kVA]
ε	The absolute error, [kWh]
δ	The percentage error, [%]

Appendix A

Table A1. The allocation on pillar, phase, and the type of the consumers.

Pillar	Branching		Phase			Consumers Type			Pillar	Branching		Phase			Consumers Type		
	1-P	3-P	a	b	c	1	2	3		1-P	3-P	a	b	c	1	2	3
1	1	-	-	1	-	1	-	-	96	1	1	1	2	1	1	-	-
2	2	-	-	2	-	1	-	-	97	1	-	-	1	-	1	-	-
3	4	-	-	4	-	1	-	-	98	1	-	-	1	-	1	-	-
4	3	-	1	2	-	1	-	-	99	6	-	-	4	2	1	-	-
7	3	-	-	3	-	1	-	-	100	4	-	-	3	1	1	-	-
8	2	-	-	2	-	1	-	-	101	1	-	-	1	-	1	-	-
9	2	-	-	2	-	1	-	-	102	3	-	-	3	-	1	-	-
10	3	-	2	1	-	1	-	-	103	1	-	-	1	-	1	-	-
11	1	-	-	1	-	1	-	-	104	1	-	-	1	-	1	-	-
12	2	-	-	2	-	1	-	-	106	2	-	1	-	1	1	-	-
13	1	-	-	1	-	1	-	-	107	3	-	1	-	2	1	-	-
14	2	-	-	-	2	1	-	-	109	1	-	-	-	1	1	-	-
15	2	-	-	1	1	1	-	-	110	1	-	-	-	1	1	-	-
17	-	1	1	1	1	1	-	-	111	3	-	-	-	3	1	-	-
18	2	-	-	-	2	1	-	-	112	4	-	-	-	4	1	-	-
19	2	-	2	-	-	1	-	-	113	1	-	-	-	1	1	-	-
20	2	-	2	-	-	1	-	-	114	3	-	-	-	3	1	-	-
21	1	-	1	-	-	1	-	-	115	1	-	-	-	1	2	-	-
22	2	-	1	1	-	1	-	-	116	1	-	-	-	1	2	-	-
23	2	-	2	-	-	1	-	-	117	-	1	1	1	1	1	-	-
24	1	-	-	-	1	1	-	-	118	-	1	1	1	1	2	-	-
26	2	-	-	-	2	1	-	-	119	1	-	1	-	-	1	-	-
27	3	-	1	-	2	1	-	-	120	1	-	1	-	-	1	-	-
28	2	-	-	1	1	1	-	-	121	2	-	2	-	-	1	-	-
29	4	-	-	1	3	1	-	-	122	2	-	1	1	-	1	-	-
30	2	-	-	-	2	1	-	-	123	4	1	2	3	1	1	-	-
31	2	-	-	-	2	1	-	-	124	3	-	2	1	-	1	-	-
32	1	-	-	-	1	1	-	-	125	2	-	-	2	-	1	-	-
33	4	-	-	-	4	1	-	-	126	2	-	-	2	-	1	-	-
34	5	-	-	-	5	1	-	-	127	2	-	1	-	1	1	-	-
35	4	-	1	1	2	1	-	-	128	2	-	2	-	-	1	-	-
36	1	-	-	1	-	1	-	-	129	4	-	4	-	-	1	-	-
37	3	-	-	-	3	1	-	-	130	1	-	-	1	-	1	-	-
38	1	-	-	-	1	1	-	-	131	3	-	-	3	-	1	-	-
39	4	-	-	1	3	1	-	-	133	2	-	1	1	-	1	-	-
40	3	-	-	-	3	1	-	-	134	1	-	-	1	-	1	-	-
41	1	-	-	-	1	1	-	-	135	3	-	3	-	-	1	-	-
42	1	-	-	-	1	1	-	-	136	3	-	3	-	-	1	-	-
43	2	-	-	-	2	1	-	-	137	3	-	-	3	-	1	-	-

Table A1. *Cont.*

Pillar	Branching		Phase			Consumers Type			Pillar	Branching		Phase			Consumers Type		
	1-P	3-P	a	b	c	1	2	3		1-P	3-P	a	b	c	1	2	3
44	2	-	-	1	1	1	-	-	138	2	-	-	2	-	1	-	-
45	4	-	-	-	4	1	-	-	139	1	-	-	1	-	1	-	-
46	2	-	-	-	2	1	-	-	140	3	1	2	3	1	1	-	-
47	3	-	1	2	-	1	-	-	141	4	-	1	3	-	1	-	-
48	3	-	1	2	-	1	2	-	142	1	-	1	-	-	1	-	-
49	2	-	-	2	-	1	-	-	143	2	-	1	1	-	1	-	-
50	1	-	-	-	1	1	-	-	144	2	-	1	1	-	1	-	-
51	1	-	-	1	-	-	2	-	145	2	-	1	-	1	1	-	-
52	3	-	-	3	-	1	2	-	146	2	-	1	1	-	1	-	-
53	1	-	-	1	-	-	2	-	147	1	-	-	1	-	1	-	-
54	6	-	-	-	6	1	2	-	148	2	-	-	1	1	1	-	-
55	2	-	1	1	-	1	-	-	149	1	-	1	-	-	1	-	-
56	2	-	-	2	-	1	-	-	150	3	-	-	2	1	1	-	-
57	1	-	-	1	-	1	-	-	151	2	-	1	1	-	1	-	-
58	1	-	1	-	-	1	-	-	152	3	-	1	2	-	1	-	-
59	2	-	-	2	-	1	-	-	153	1	-	1	-	-	1	-	-
60	2	-	1	1	-	1	-	-	154	1	-	1	-	-	1	-	-
61	1	-	-	1	-	1	-	-	155	2	-	2	-	-	1	-	-
62	1	-	-	-	1	1	-	-	156	2	-	-	1	1	1	-	-
63	2	-	2	-	-	1	-	-	157	2	-	1	1	-	1	-	-
65	1	-	-	1	-	1	-	-	158	2	-	1	1	-	1	-	-
66	4	-	1	3	-	1	-	-	159	1	-	-	1	-	1	-	-
67	2	-	-	2	-	1	-	-	161	1	-	1	-	-	1	-	-
68	2	-	-	2	-	1	-	-	162	2	-	-	2	-	1	-	-
69	2	-	1	1	-	1	-	-	163	1	-	-	-	1	1	-	-
70	1	-	-	1	-	1	-	-	164	3	-	2	-	1	1	-	-
71	1	-	-	1	-	1	-	-	165	1	-	1	-	-	1	-	-
72	1	-	-	1	-	1	-	-	166	2	-	1	-	1	1	-	-
75	2	-	-	2	-	1	-	-	168	2	-	2	-	-	1	-	-
76	2	-	-	2	-	1	-	-	169	3	-	2	-	1	1	-	-
77	2	-	1	1	-	1	-	-	170	1	-	1	-	-	1	-	-
78	4	-	1	3	-	1	-	-	171	2	-	-	-	2	1	-	-
79	1	1	1	2	1	1	-	-	172	2	-	-	1	1	1	-	-
80	2	-		2	-	1	-	-	173	2	1	2	1	2	1	-	-
82	2	-	-	2	-	1	-	-	174	2	-	1	-	1	1	-	-
83	1	-	1	-	-	1	-	-	175	2	-	-	-	2	1	-	-
84	2	-	-	2	-	1	-	-	176	2	-	1	-	1	1	-	-
86	1	-	-	1	-	1	-	-	177	2	-	1	-	1	1	-	-
87	2	-	-	2	-	1	-	-	179	1	-	-	-	1	1	-	-
88	1	-	-	1	-	1	-	-	180	1	-	1	-	-	1	-	-
89	2	-	-	2	-	1	-	-	181	1	-	-	-	1	1	-	-

Table A1. *Cont.*

Pillar	Branching		Phase			Consumers Type			Pillar	Branching		Phase			Consumers Type		
	1-P	3-P	a	b	c	1	2	3		1-P	3-P	a	b	c	1	2	3
90	1	-	-	1	-	1	-	-	183	1	-	-	-	1	1	-	-
91	2	-	-	2	-	1	-	-	184	1	-	-	-	1	1	-	-
92	1	-	-	1	-	1	-	-	185	1	-	-	1	-	1	-	-
93	2	-	-	2	-	1	-	-	187	1	-	1	-	-	1	-	-
94	1	-	1	-	-	1	-	-	188	1	-	1	-	-	1	-	-
95	1	-	-	1	-	1	-	-	189	1	-	-	-	1	1	-	-

Table A2. The energy losses calculated with proposed algorithm—Feeder 1, [kWh].

Hour	Main Conductors				Branching Conductors				Total
	a	b	c	Neutral	a	b	c	Neutral	
1	0	0.002018	0	0.002518	0	0.000253	0	0.000166	0.004955
2	0	0.00142	0	0.001774	0	0.000175	0	0.000115	0.003484
3	0	0.001438	0	0.001797	0	0.000176	0	0.000115	0.003527
4	0	0.001555	0	0.001947	0	0.000189	0	0.000124	0.003815
5	0	0.0012	0	0.001499	0	0.000145	0	9.53e-05	0.00294
6	0	0.001208	0	0.001508	0	0.000146	0	9.58e-05	0.002958
7	0	0.0015	0	0.001867	0	0.000183	0	0.00012	0.00367
8	0	0.00154	0	0.001916	0	0.000189	0	0.000124	0.003768
9	0	0.001351	0	0.001679	0	0.000174	0	0.000114	0.003317
10	0	0.001747	0	0.002171	0	0.000225	0	0.000148	0.004291
11	0	0.001319	0	0.00164	0	0.000167	0	1.10e-04	0.003237
12	0	0.001761	0	0.002189	0	0.000227	0	0.000149	0.004326
13	0	0.001889	0	0.002347	0	0.000245	0	0.000161	0.004641
14	0	0.001428	0	0.001771	0	0.000185	0	0.000121	0.003505
15	0	0.001427	0	0.001773	0	0.000185	0	0.000121	0.003506
16	0	0.001832	0	0.002273	0	0.000236	0	0.000155	0.004497
17	0	0.00184	0	0.002271	0	0.000255	0	0.000167	0.004533
18	0	0.001808	0	0.002231	0	0.000247	0	0.000162	0.004448
19	0	0.002043	0	0.002524	0	0.000277	0	0.000181	0.005026
20	0	0.00227	0	0.002808	0	0.000312	0	0.000205	0.005595
21	0	0.003143	0	0.003882	0	0.000443	0	0.00029	0.007758
22	0	0.004848	0	0.005993	0	0.000661	0	0.000433	0.011936
23	0	0.004099	0	0.005075	0	0.000568	0	0.000372	0.010114
24	0	0.002171	0	0.002703	0	0.000268	0	0.000176	0.005318
Total	0	0.046854	0	0.058157	0	0.006134	0	0.00402	0.115165

Table A3. The energy losses calculated with proposed algorithm—Feeder 2, [kWh].

Hour	Main Conductors				Branching Conductors				Total
	a	b	c	Neutral	a	b	c	Neutral	
1	0.0201	0.4897	0.1064	0.3975	0.0019	0.0103	0.0008	0.0085	1.0350
2	0.0145	0.3723	0.0782	0.3027	0.0014	0.0084	0.0006	0.0068	0.7848
3	0.0139	0.3780	0.0837	0.3103	0.0011	0.0086	0.0006	0.0068	0.8030
4	0.0149	0.4240	0.0879	0.3472	0.0013	0.0102	0.0006	0.0079	0.8940
5	0.0122	0.3414	0.0728	0.2799	0.0010	0.0083	0.0005	0.0064	0.7226
6	0.0129	0.3174	0.0776	0.2614	0.0011	0.0067	0.0006	0.0055	0.6833
7	0.0190	0.3678	0.0983	0.3005	0.0019	0.0065	0.0007	0.0060	0.8008
8	0.0213	0.3475	0.0993	0.2827	0.0025	0.0053	0.0008	0.0056	0.7648
9	0.0172	0.2792	0.0716	0.2236	0.0021	0.0042	0.0006	0.0045	0.6030
10	0.0206	0.3828	0.0930	0.3076	0.0022	0.0065	0.0007	0.0062	0.8197
11	0.0164	0.3121	0.0734	0.2506	0.0019	0.0056	0.0006	0.0053	0.6659
12	0.0194	0.4158	0.0902	0.3339	0.0020	0.0081	0.0007	0.0071	0.8774
13	0.0226	0.4602	0.0966	0.3671	0.0026	0.0091	0.0007	0.0081	0.9670
14	0.0163	0.3305	0.0772	0.2664	0.0016	0.0061	0.0006	0.0055	0.7042
15	0.0159	0.3303	0.0738	0.2654	0.0017	0.0062	0.0006	0.0056	0.6995
16	0.0205	0.4027	0.1010	0.3263	0.0020	0.0070	0.0008	0.0064	0.8666
17	0.0222	0.4306	0.0886	0.3414	0.0025	0.0083	0.0007	0.0075	0.9019
18	0.0228	0.4079	0.0920	0.3241	0.0026	0.0072	0.0008	0.0069	0.8642
19	0.0257	0.3984	0.1046	0.3184	0.0029	0.0057	0.0008	0.0062	0.8628
20	0.0292	0.3904	0.1056	0.3099	0.0037	0.0048	0.0009	0.0061	0.8506
21	0.0373	0.4999	0.1377	0.3974	0.0044	0.0058	0.0011	0.0074	1.0911
22	0.0519	0.7618	0.2340	0.6188	0.0050	0.0085	0.0019	0.0100	1.6919
23	0.0407	0.7067	0.1783	0.5657	0.0040	0.0099	0.0014	0.0100	1.5168
24	0.0217	0.4255	0.1328	0.3558	0.0016	0.0062	0.0010	0.0058	0.9505
Total	0.5294	9.9731	2.4546	8.0549	0.0549	0.1735	0.0191	0.1621	21.4215

Table A4. The energy losses calculated with proposed algorithm—Feeder 3, [kWh].

Hour	Main Conductors				Branching Conductors				Total
	a	b	c	Neutral	a	b	c	Neutral	
1	0.2724	0.2458	0.2612	0.0673	0.0031	0.0025	0.0026	0.0035	0.8582
2	0.1935	0.1774	0.1897	0.0475	0.0022	0.0018	0.0019	0.0025	0.6165
3	0.1849	0.1788	0.1940	0.0464	0.0021	0.0018	0.0020	0.0024	0.6123
4	0.2051	0.1948	0.2117	0.0512	0.0024	0.0020	0.0022	0.0026	0.6719
5	0.1583	0.1535	0.1666	0.0394	0.0018	0.0015	0.0017	0.0020	0.5249
6	0.1580	0.1549	0.1668	0.0392	0.0018	0.0015	0.0017	0.0021	0.5258
7	0.2129	0.1937	0.2020	0.0506	0.0025	0.0018	0.0020	0.0029	0.6684
8	0.2373	0.2054	0.2011	0.0549	0.0029	0.0020	0.0019	0.0033	0.7088
9	0.2023	0.1654	0.1649	0.0482	0.0024	0.0017	0.0015	0.0028	0.5892
10	0.2445	0.2059	0.2120	0.0592	0.0028	0.0020	0.0019	0.0033	0.7317
11	0.1882	0.1584	0.1632	0.0450	0.0022	0.0015	0.0015	0.0026	0.5626
12	0.2395	0.2037	0.2130	0.0586	0.0027	0.0020	0.0020	0.0032	0.7246

Table A4. *Cont.*

Hour	Main Conductors				Branching Conductors				Total
	a	b	c	Neutral	a	b	c	Neutral	
13	0.2684	0.2191	0.2275	0.0653	0.0031	0.0021	0.0021	0.0036	0.7913
14	0.1870	0.1620	0.1727	0.0461	0.0020	0.0015	0.0016	0.0025	0.5754
15	0.1907	0.1627	0.1706	0.0466	0.0021	0.0016	0.0016	0.0026	0.5784
16	0.2372	0.2082	0.2198	0.0584	0.0026	0.0019	0.0020	0.0032	0.7333
17	0.2506	0.2007	0.2141	0.0632	0.0028	0.0019	0.0018	0.0036	0.7387
18	0.2505	0.2025	0.2133	0.0625	0.0028	0.0019	0.0018	0.0036	0.7389
19	0.2839	0.2279	0.2396	0.0706	0.0033	0.0021	0.0020	0.0040	0.8334
20	0.3297	0.2479	0.2627	0.0829	0.0040	0.0024	0.0023	0.0047	0.9366
21	0.4392	0.3315	0.3553	0.1130	0.0051	0.0032	0.0030	0.0062	1.2564
22	0.6306	0.5135	0.5523	0.1628	0.0067	0.0047	0.0047	0.0085	1.8838
23	0.5370	0.4351	0.4719	0.1395	0.0057	0.0042	0.0040	0.0072	1.6047
24	0.2686	0.2618	0.2799	0.0676	0.0028	0.0024	0.0027	0.0035	0.8892
Total	6.3702	5.4105	5.7257	1.5859	0.0718	0.0520	0.0524	0.0865	19.3550

Table A5. The phase voltages at the farthest pillars (P95 and P188), calculated cu both algorithms [V].

Hour	Pillar P95						Pillar P188					
	PA			PFDS			PFDS			PFDS		
	a	b	c	a	b	c	a	b	c	a	b	c
1	228.81	216.95	229.17	228.72	216.34	229.04	216.05	217.82	216.03	215.85	218.48	215.70
2	228.92	218.59	229.20	228.83	218.45	229.10	218.20	219.56	218.12	218.11	220.23	218.22
3	229.89	219.45	230.09	229.81	218.26	229.99	219.39	220.40	218.92	219.34	221.08	219.01
4	231.04	220.02	231.27	230.97	219.64	231.16	219.97	221.15	219.68	219.92	221.86	219.74
5	232.20	222.31	232.39	232.13	221.26	232.29	222.54	223.42	222.11	222.53	224.11	222.39
6	234.37	224.80	234.56	234.30	223.86	234.46	224.75	225.55	224.22	224.73	226.22	224.46
7	234.44	224.16	234.78	234.35	223.10	234.64	223.37	224.73	223.24	223.22	225.37	223.21
8	231.03	221.04	231.46	230.90	220.80	231.31	219.37	221.13	219.82	219.04	221.66	219.64
9	229.33	220.39	229.82	229.20	219.83	229.69	218.50	220.52	219.03	218.15	221.03	218.99
10	228.06	217.59	228.54	227.89	217.08	228.36	216.09	218.15	216.30	215.44	218.47	215.68
11	228.54	219.11	228.97	228.39	218.79	228.82	218.09	219.85	218.29	217.57	220.21	218.04
12	227.88	216.99	228.34	227.71	216.49	228.16	215.98	217.98	216.09	215.29	218.26	215.41
13	227.60	216.19	228.15	227.41	215.65	227.95	215.05	217.43	215.45	214.22	217.65	214.61
14	227.93	218.20	228.33	227.77	217.91	228.16	217.46	219.08	217.23	216.90	219.39	216.81
15	228.21	218.49	228.62	228.05	218.20	228.46	217.60	219.35	217.58	217.03	219.66	217.20
16	227.25	216.49	227.68	227.08	216.06	227.47	215.43	217.18	215.14	214.72	217.42	214.30
17	226.95	215.94	227.57	226.76	215.43	227.38	214.90	217.34	214.97	214.12	217.60	214.15
18	226.79	216.05	227.40	226.62	215.46	227.22	214.78	217.14	214.87	214.10	217.46	214.15
19	226.92	216.25	227.56	226.76	215.46	227.38	214.10	216.65	214.28	213.47	217.06	213.50
20	226.10	215.56	226.89	225.96	215.51	226.72	212.28	215.53	212.96	211.68	216.05	212.21
21	226.01	214.06	226.90	225.86	212.51	226.71	209.95	213.77	210.61	209.17	214.25	209.18
22	221.99	207.14	222.81	221.84	206.00	222.51	202.55	206.42	202.70	201.45	206.58	201.50
23	224.20	209.92	224.98	224.06	209.50	224.75	206.21	209.91	206.49	205.34	210.25	205.22
24	227.82	216.61	228.06	227.71	215.31	227.88	215.16	216.30	214.37	214.90	216.84	213.70

References

1. Grigoras, G. Impact of smart meter implementation on saving electricity in distribution networks in Romania. In *Application of Smart Grid Technologies. Case Studies in Saving Electricity in Different Parts of the World*; Lamont, L.A., Sayigh, A., Eds.; Academic Press: Cambridge, MA, USA, 2018; pp. 313–346.
2. Hierzinger, R.; Albu, M.; Van Elburg, H.; Scott, A.; Łazicki, A.; Penttinen, L.; Puente, F.; Sæle, H. European Smart Metering Landscape Report (IEE). 2013. Available online: https://ec.europa.eu/energy/intelligent/projects/sites/iee-projects/files/projects/documents/smartregions_landscape_report_2012_update_may_2013.pdf (accessed on 12 June 2019).
3. Žádník, J. Cost Benefit Studies (CBA) for Smart Metering Roll-Out in the EU, Overview and Way Forward, Smart Grids in Practice. 29 September 2015. Available online: http://kampan.snt.sk/OSGP/prezentacie/PWC%202015_09_29_%20OSGP%20Slovakia%20Josef%20Zadnik.pdf (accessed on 12 June 2019).
4. Institute of Communication & Computer Systems of the National Technical University of Athens ICCS-NTUA for European Commission. Study on Cost Benefit Analysis of in EU Member States Smart Metering Systems, Final Report. 25 June 2015. Available online: https://ec.europa.eu/energy/en/content/study-cost-benefit-analysis-smart-metering-systems-eu-member-states (accessed on 12 June 2019).
5. European Commission. Smart Metering Deployment in the European Union. Available online: http://ses.jrc.ec.europa.eu/smart-metering-deployment-european-union (accessed on 12 June 2019).
6. European Commission, Directorate-General for Energy. Standardization Mandate to CEN, CENELEC, and ETSI in the Field of Measuring Instruments for the Developing of an Open Architecture for Utility Meters Involving Communication Protocols Enabling Interoperability, M 441/EN. 2009. Available online: https://ec.europa.eu/energy/sites/ener/files/documents/2011_03_01_mandate_m490_en.pdf (accessed on 12 June 2019).
7. European Commission, Directorate-General for Energy, Standardization Mandate to European Standardisation Organisations (ESOs) to Support European Smart Grid Deployment, M/490 EN. 2016. Available online: https://ec.europa.eu/energy/sites/ener/files/documents/2011_03_01_mandate_m490_en.pdf (accessed on 12 June 2019).
8. Leonardo, M.; Queiroz, O.; Marcio, A.; Roselli, A.; Cavellucci, C.; Lyra, C. Energy Losses Estimation in Power Distribution Systems. *IEEE Trans. Power Syst.* **2012**, *27*, 1879–1887.
9. Nassim, I.; Basa, A.; Çakir, B. A Simple Method to Estimate Power Losses in Distribution Networks. In Proceedings of the 10th International Conference on Electrical and Electronics Engineering (ELECO), Bursa, Turkey, 30 November–2 December 2017.
10. Yusoff, M.; Busrah, A.; Mohamad, M.; Au, M.T. A Simplified Approach in Estimating Technical Losses in TNB Distribution Network Based on Load Profile and Feeder Characteristics. *Recent Adv. Manag. Mark. Financ.* **2010**, *15*, 99–105.
11. Raesaar, P.; Tiigimagi, E.; Valtin, J. Strategy for Analysis of Loss Situation and Identification of Loss Sources in Electricity Distribution Networks. *Oil Shale* **2007**, *24*, 297–307.
12. Bunluesak, K.; Horkierti, J.; Kaewtrakulpong, P. Power Loss Estimation in Distribution System A Case Study of PEA Central Area I. Available online: http://www.ecti-thailand.org/assets/papers/412_pub_24.pdf (accessed on 12 June 2019).
13. Au, M.T.; Tan, C.H. Energy flow models for the estimation of technical losses in distribution network. In Proceedings of the 4th International Conference on Energy and Environment, Putrajaya, Malaysia, 5–6 March 2013.
14. Feng, N.; Jianming, Y. Low-Voltage Distribution Network Theoretical Line Loss Calculation System Based on Dynamic Unbalance in Three Phrases. In Proceedings of the 2010 International Conference on Electrical and Control Engineering, Wuhan, China, 25–27 June 2010.
15. Celli, G.; Natale, N.; Pilo, F.; Pisano, G.; Bignucolo, F.; Coppo, M.; Savio, A.; Turri, R.; Cerretti, A. Containment of power losses in LV networks with high penetration of distributed generation. *CIRED Open Access Proc. J.* **2017**, *2017*, 2183–2187. [CrossRef]
16. Mikic, O.M. Variance-based energy loss computation in low voltage distribution networks. *IEEE Trans. Power Syst.* **2017**, *22*, 179–187. [CrossRef]
17. Ogunjuyigbe, A.S.O.; Ayodele, T.R.; Akinola, O.O. Impact of distributed generators on the power loss and voltage profile of sub-transmission network. *J. Electr. Syst. Inf. Technol.* **2016**, *3*, 94–107. [CrossRef]

18. Zolkifri, N.I.; Gan, C.K.; Khamis, A.; Baharin, K.A.; Lada, M.Y. Impacts of residential solar photovoltaic systems on voltage unbalance and network losses. In Proceedings of the TENCON 2017—2017 IEEE Region 10 Conference, Penang, Malaysia, 5–8 November 2017.
19. Gawlak, A.; Poniatowski, L. Power and energy losses in low-voltage overhead lines with prosumer microgeneration plants. In Proceedings of the 18th International Scientific Conference on Electric Power Engineering (EPE), Kouty nad Desnou, Czech Republic, 17–19 May 2017.
20. Ramesh, L.; Chowdhury, S.P.; Chowdhury, S.; Natarajan, A.A.; Gaunt, C.T. Minimization of power loss in distribution networks by different techniques. *Int. J. Electr. Power Energy Syst. Eng.* **2009**, *2*, 1–6.
21. Dashtaki, A.K.; Haghifam, M.R. A New Loss Estimation Method in Limited Data Electric Distribution Networks. *IEEE Trans. Power Deliv.* **2013**, *28*, 2194–2200. [CrossRef]
22. Grigoras, G.; Cartina, G.; Istrate, M.; Rotaru, F. The Efficiency of the Clustering Techniques in the Energy Losses Evaluation from Distribution Networks. *Int. J. Math. Models Methods Appl. Sci.* **2011**, *5*, 133–141.
23. Wang, S.; Dong, P.; Tian, Y. A Novel Method of Statistical Line Loss Estimation for Distribution Feeders Based on Feeder Cluster and Modified XGBoost. *Energies* **2017**, *10*, 2067. [CrossRef]
24. Fernandes, C.M.M. Unbalance between Phases and Joule's Losses in Low Voltage Electric Power Distribution. Available online: Fenix.tecnico.ulisboa.pt/downloadFile/395142112117/Resumo20Alargado%20Carlos%20Fernandes.pdf (accessed on 11 June 2019).
25. Rupa, J.M.; Ganesh, S. Power flow analysis for radial distribution system using backward/forward sweep method. *Int. J. Electr. Comput. Electron. Commun. Eng.* **2014**, *8*, 1540–1544.
26. Madjissembaye, N.; Muriithi, C.M.; Wekesa, C.W. Load Flow Analysis for Radial Distribution Networks Using Backward/Forward Sweep Method. *J. Sustain. Res. Eng.* **2017**, *3*, 82–87.
27. Janecek, E.; Georgiev, D. Probabilistic extension of the backward/forward load flow analysis method. *IEEE Trans. Power Syst.* **2011**, *27*, 695–704. [CrossRef]
28. Eremia, M.; Tristiu, I. Radial and Meshed Networks. In *Electric Power Systems. Electric Networks*; Eremia, M., Ed.; House of Romanian Academy: Bucharest, Romania, 2006; pp. 83–164.
29. Grigoras, G.; Gavrilas, M. An Improved Approach for Energy Losses Calculation in Low Voltage Distribution Networks based on the Smart Meter Data. In Proceedings of the International Conference and Exposition on Electrical and Power Engineering (EPE), Iasi, Romania, 18–19 October 2018.
30. Kriukov, A.; Vicol, B.; Gavrilas, M.; Ivanov, O. A Stochastic Method for Calculating Energy Losses in Low Voltage Distribution Networks Using Genetic Algorithms. *AGIR Bull.* **2012**, *3*, 595–602.